Materials Research. 2026; 29: e20250709
DOI: https://doi.org/10.1590/1980-5373-MR-2025-0709

An Investigation of T6 Heat Treatment, and Corrosion Behaviour of AA7085/TiB_2 Composites

V. Karunanithi[a], *A. Arockia Julias*[a*], *P. Loganathan*[b]

[a]*B.S. Abdur Rahman Crescent Institute of Science and Technology, Department of Mechanical Engineering, Chennai, India.*
[b]*SRM Institute of Science and Technology, Department of Mechanical Engineering, Ramapuram Campus, Chennai, India.*

Received: November 6, 2025; Revised: February 10, 2026; Accepted: March 8, 2026

There is potential to improve corrosion resistance of AA7085 aluminium alloy by adding ultra-high temperature ceramic particles such as TiB_2 and by using better T6 ageing conditions. AA7085 composites with 3–9 wt.% TiB_2 particles were fabricated by the stir-casting method. T6 heat treatment of 525 °C solutionising, then artificial ageing at 230 °C for 10 hours was performed. Hardness assessment, 3.5 wt.% NaCl immersion corrosion for 24 hours, 48 hours and 72 hours, and Optical microscopy and SEM analysis studies as indicates the fine distribution of TiB2 particles. The AT9 sample achieved a maximum hardness of 122 HV, about 35% higher than the base AA7085. The lowest corrosion rate was observed for the AT9 composite at 230 °C ageing rate of 0.12 mm yr^{-1} at 72 hours. TiB_2 particles inhibited pit initiation and promoted the formation of an Al-rich passivation layer. At higher ageing, pitting was observed to increase due to the reduction of over-ageing precipitates. The AA7085 composite reinforced with 9 wt.% TiB_2 and artificially aged at 230 °C improved the corrosion resisting behaviour. The TiB_2-Al matrix interface and the formation of a dense passivation layer are the key mechanisms for the enhanced corrosion resistance process.

Keywords*: Corrosion, Hard ceramics, SEM, Hardness, Heat Treatment.*

1. Introduction

The composite materials which are newly derived using aluminum as a base material exhibit better properties, that include higher strength and remarkable thermal conductivity, along with their well-known lower density. These properties transform them suitable for a varied set of industrial applications. Cylinder block liners, automotive pistons, and bicycle frames are among the numerous engineering applications of aluminum-based composites[1]. The 7xxx series of aluminium alloys is especially significant among all of the series due to its great strength. These alloys are mostly used in aircraft constructions owing to their superior characteristics and lightweight nature. However, these alloy inadequate capacity to withstand corrosion limits their overall significance[2].

Because the Zn-rich Al alloy has excellent mechanical properties, AA7xxx series with higher zinc content is becoming an increasingly popular choice among aluminium alloys as matrix material[3]. To improve the stiffness and strength of the bulk material's matrix, reinforcement is utilised as particulate-reinforced metal matrix composites (MMCs). The addition of individual particles eliminates the complications in the preparation of continuously aligned metal matrix composites (MMCs) and the low interfacial response[4]. The incorporation of ceramic particles such as Al_2O_3, TiB_2, B_4C, and SiC to aluminium matrix composites enhances their mechanical and corrosion resistance properties. Among these, TiB_2 is selected because it has high hardness, high elastic modulus, high melting point, and better temperature stability[5].

Several preparation methods are used to produce MMCs, including solid-state deposition in the form of particles or powders, molten liquid, and various deposition technologies[6]. The stir casting method has several advantages over other manufacturing methods, such as simplicity, adaptability to a wide range of materials, high production rate, and low cost, making it ideal for large-scale composite production[7,8]. Furthermore, secondary processes such as heat treatment ensure excellent properties of the composites; it improves mechanical properties by forming small, stabilised precipitates and inhibiting dislocation motion[9].

The integrity of the oxide layer that shall form initially in the matrix material, which is intended to protect the material from initial corrosion attacks can be compromised by reinforcement[10]. Several researchers have highlighted additional factors that influence corrosion resistivity, including heat treatment, the type of reinforcements used, and the levels of reinforcement applied[11]. Suthar and Patel[12] examined the corrosion performance of pure aluminium material reinforced with Mg/Gr/Ti/B_4C hybrid composites. The composites with increased particularly boron carbide (B_4C) and graphite, demonstrate the highest corrosion rates among all evaluated solutions. It results from the way carbon molecules activity as a cathode in galvanic cells that form on composite materials' surfaces. The behaviour of AA7475/CSA/Gr composites in terms of immersion corrosion was investigated by Kadaru et al.[13].

*e-mail: *juliasarok@gmail.com*
Associate Editor: José Daniel Biasoli de Mello.
Editor-in-Chief: Luiz Antonio Pessan.

The rate of corrosion reduces when they increased the quantity of graphite (Gr) in the hybrid composite after 240 hours of exposure to 8% NaCl. Mahmoud et al.[14] overseen a comprehensive investigation on the corrosion behavior of composites that consist of Pure Al/SiC and Al/Al_2O_3 fabricated through powder metallurgy techniques. Their findings indicate that the resistance offered by the material for corrosion of the composites is enhanced when the size of the ceramic nano particles SiC and Al_2O_3 increases.

Dhanapal et al.[15] indicated that the rate of corrosion observed in the experiments conducted using salt spray apparatus exceeds that of both the immersion and galvanic corrosion tests conducted on AZ61A magnesium alloy. The rate of corrosion rate of the magnesium-based alloy decreases when the pH level increases, due to the development of a hydroxide layer. He et al.[16] investigated the impact of artificial ageing on AA6082. Their findings confirm the de-dissolving sequence of ageing precipitation, indicating that the optimal ageing treatment takes place at 175°C for a duration of 8 hours. An exploration on the microstructure and mechanical properties carried out by Chen et al.[17] on ZL 104 aluminium alloy that are subjected to T6 heat treated shows that the material's strength improved, although it compromises the elongation as it decreases. Additionally, they observed that increasing the ageing period improved strength.

Dhanashekar Manickam and Senthil Kumar Velukkudi Santhanam observed the influence of artificial ageing treatment on the compressive nature of an aluminum alloy A356. The enhanced compression strength is attained during 4 hours of artificial ageing at 180°C[18]. Research on the corrosive nature of the AA7150-T651 aluminium material was performed by Liu et al.[19] and encountered that the progressive rise in open circuit potential during the transient phase is due to the decreasing proportion of the surface area occupied by the deformed layer. Sambathkumar et al.[20] performed a study on the corrosive nature of Al 7075/Al2O3/B4C composites to find the rate of corrosion by employing the potentiodynamic polarisation method in a sodium chloride solution with appropriate weight percentage. The corrosion rate of the Al 7075 hybrid composite, containing 15 volume percent reinforcement, was observed at 0.336 mm annually.

According to the findings reported by various researchers in their literatures it is noted that, integrating particles made from ceramic materials to aluminium alloys remarkably enrich their resistance to corrosion. Despite extensive research on AA7085 matrix composites, a significant gap persists in the examination of their corrosion behaviour. This is particularly apparent when analysing a limited variety of ceramics materials used as reinforcement and their heat treatment attributes.

In this study, the effects of different ageing temperatures and ultrahigh-temperature ceramic (UHTC) on the composition of AA7085 aluminium alloy reinforced with TiB_2 particles are investigated. The composite was fabricated by stir casting with various weight per cent additions of TiB_2 of AA7085. Then, the composite was heat treated with T4 and T6 conditions. The properties of the prepared composites and base AA7085 aluminium were evaluated by conducting a capillary tube test in NaCl solution. The exposure times for the samples ranged from 24 to 72 hours. The mass loss was measured in order to determine the materials' rate of corrosion. Scanning electron microscopy (SEM) was used to evaluate the corroded surfaces and the images were used to analyse the corrosion mechanism.

2. Materials and Method

This work utilized AA7085 aluminium alloy as the matrix and its chemical composition as shown in Table 1. The TiB_2 reinforcing particles had a purity level of around 99.5%. SEM analysis revealed that the particles exhibited irregular morphology as shown in Figure 1(a). Figure 1(b) indicate XRD phase analysis of TiB_2 particles with (111) at 36.52°, (200) at 42.479°, (220) at 61.736°, (311) at 74.050°, and (222) at 77.934°, respectively. The chemical composition of TiB_2 particles is indicated in Table 2.

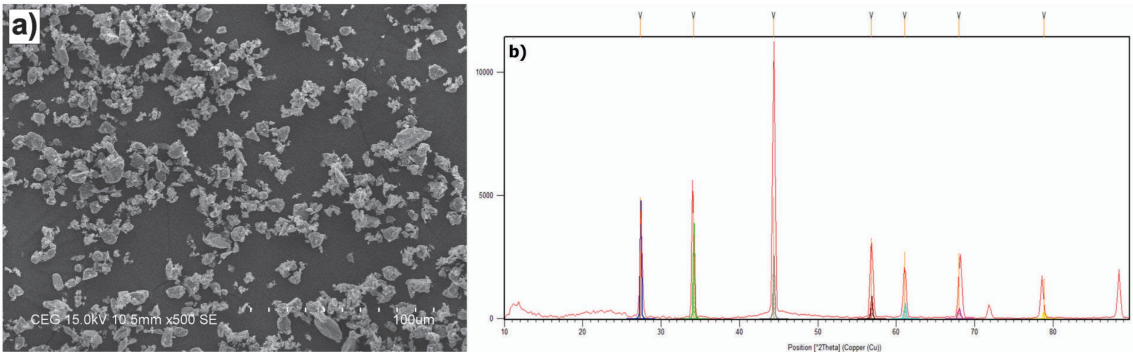

Figure 1. SEM and XRD analysis of TiB_2 Particles.

Table 1. Chemical Composition of AA7085.

Composition	Zn	Mg	Cu	Zr	Fe	Si	Al
Percentage %	7.0–8.0	1.2–1.8	1.3–2.0	0.08–0.15	≤0.08%,	≤0.06%.	Remaining

The graphite crucible had been charged with a sufficient quantity of AA7085 billets and heated to a liquidus temperature of 850 °C for a duration of 10 to 15 minutes to attain a thermal uniformity and dislocation of segregation without excessive oxidation. Preheating TiB_2 particles in a furnace at 150 °C for one hour enhanced their wettability. The solidification process is carried out in inert atmosphere to minimize the oxidization through purging of argon gas at the rate of 3-5 l/min. In order to reduce thermal shock during the pouring of molten metal, the split die is preheated for 250 °C. The preheated TiB_2 particles taken in appropriate percentage were then added to the melt slurry using a drop feed mechanism while maintaining continuous agitation at 150 RPM. The melted slurry was subjected to heating that exceeded the liquidus temperature and was subsequently agitated at 500 RPM for 2-3 minutes. This stirring process effectively prevented the reinforcement particles from floating due to the density differential between the matrix and the reinforcement.

Subsequently, the molten alloy was transferred into a preheated metal die and permit to cool in room temperature. Figure 2 shows the fabricated AT9 composite. The samples were designated as AA0, AT3, AT6, and AT9, with each designation indicating a distinct level of TiB_2 reinforcement.

2.1. Secondary process – heat treatment

The fabricated composites are subjected to T6 heat treatment process such as solution treatment carried in an electric – resistance muffle furnace, followed by water quenching at room temperature and then artificial ageing. The solution treatment was carried out at 525 °C at a regulated heating rate of 1.5 °C/h for 2 hr. After the solution heat treatment, the specimen was water quenched at room temperature. To avoid natural aging prior to artificial ageing. The artificial ageing was carried out respectively at 230 °C for 10 hrs. The heat treatment process carried out in argon atmosphere conditions.

2.2. Microstructure and phase analysis

The specimens were subjected to metallographic polishing utilizing various grades of silicon carbide (SiC) abrasive papers and etched using the conventional Keller's reagent. Following, a morphology assessment was conducted using optical microscope and Scanning Electron Microscope (SEM) and chemical composition are analyzed via Energy Dispersive Analysis (EDS). The Phase analysis of fabricated alloy and composites are further analysis through X-Ray diffraction.

2.3. Microhardness

The microhardness was carried out in solution treated, quenched and artificial ageing condition alloy and composites was evaluated using a Vickers hardness tester in accordance with ASTM E384-16. A constant load of 500g was applied to each indentation with a dwell period of 15 seconds. Hardness measurements were performed at multiple locations, carefully in the aluminium matrix, TiB_2 particles, and matrix–particle interfaces, to identify the differences in local mechanical properties.

2.4. Immersion corrosion test

The immersion corrosion test carried out on alloy and composites at artificial ageing at 230°C conditions. Prior to testing, the sample surfaces were progressively polished using varying emery paper grades to achieve a smooth surface. To prevent contamination, distilled water was also used to thoroughly clean each test beaker. The test specimens utilised in the study are displayed in Figure 3. The pH of the solution is maintained at 7.5, as measured by a pH meter, with all tests performed at room temperature (22 – 24 °C) under static immersion conditions with immersion durations of 24, 48, and 72 hours. To provide a constant corrosive environment and prevent concentration fluctuations from evaporation or the formation of corrosion products, the NaCl solution was regularly maintained at scheduled times throughout the exposure time. Before immersing the samples in the NaCl solution, they were adequately rinsed with distilled water and soaked in methanol. The weight of the individual sample at higher accuracy was carefully recorded before and after each experiment to find out the amount of weight loss.

Figure 2. Fabricated AA7085/TiB_2 composite.

Figure 3. Samples immersed in corrosion medium.

Table 2. Chemical Composition of TiB_2 Particles.

Ti	B	N	Si	Fe	Ni
>65.45	>29.55	<0.09	<0.14	<0.08	<0.01

The weight loss that was measures was then used to calculate the corrosion rate based on Equation (1). The corroded samples are examined under SEM.

$$Corrosion\ rate\ \left(mm / year\right) = \frac{KW}{ADT} \quad (1)$$

$K = 8.76\,x10^4;\ T - Time,$

$A - Area\ of\ the\ samples,$

$W - weight\ loss,\ D - Density$

3. Results And Discussion

3.1. Microstructure analysis

The images obtained by subjecting the AA7085 alloy and TiB_2 reinforced composites into optical microscopic investigation under as casted condition, solutioning and artificial aging are shown in Figure 4. The casting exhibits no flaws and possesses a uniform grain structure. The micrographs depict the α-phase (white) rich in aluminium, the η-phase (black) abundant in zinc, and the intermetallic phases located within grains and along boundaries.

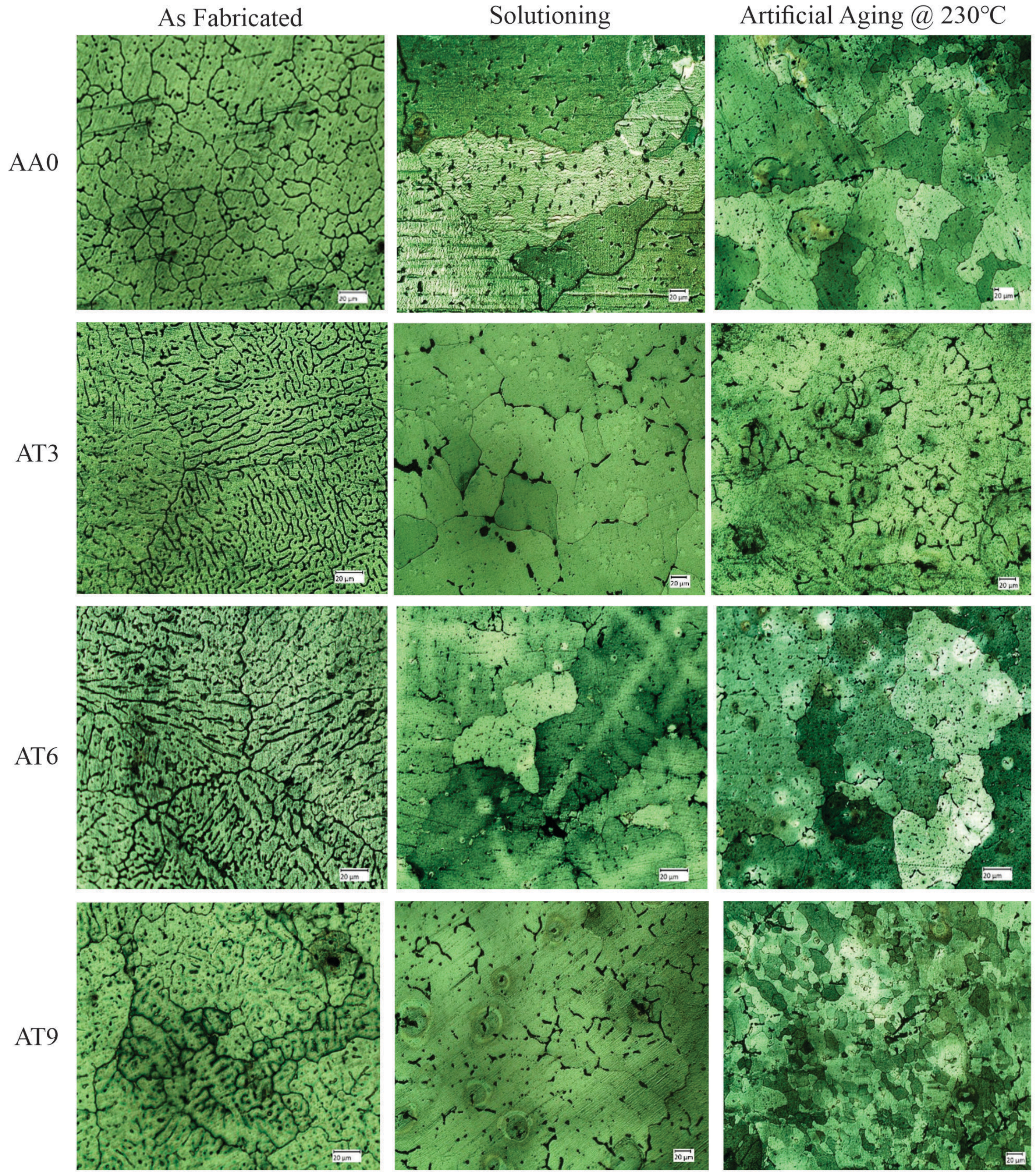

Figure 4. Heat Treated alloy and composites at different aging temperature

The uniform dispersion of ceramic particles acting as nucleation sites is responsible for the heat-treated materials' equiaxed and refined grain structure[21].

The artificial gaining conditions for OM result in a more refined grain structure due to the uniform dispersion of particulates within the aluminum matrix. These improved microstructural properties are primarily the result of the material solidifying at a significantly higher cooling rate[22]. A non-dendritic microstructure is exhibited in the T6-treated alloy and composites, which have primary phases within and β-phase intermetallic along grain boundaries. Strong bonding between the surfaces and even distribution of the reinforcement improve adhesion, which in turn improves the mechanical qualities[23]. After undergoing the typical solution treatment, the alloy's microstructure was found to be quite homogeneous, with few precipitates concentrated at the grain boundaries. Further decrease in dislocation density and an increase in grain growth at aging condition.

The SEM and EDS analysis of the alloy and composites at 230 °C, owing to the increased hardness, and conducted analyses under elevated ageing conditions, are shown in Figure 5(a-d). The microstructural analysis revealed fine and well-bonded interfaces between the matrix and particles in both materials, with no indications of interfacial defects such as porosity, unbonding. In this regard, there were no signs of particle agglomeration or reaction products, as evidenced by the subsequent EDS, which clearly shows stability of particles within the matrix, thereby reducing corrosion with subsequent improvements in hardness. It indicates a fine distribution of particles, and the existence of TiB_2 particles is confirmed by EDS analysis. Subsequent XRD examination confirms the phase stability of α-Al and TiB_2 particles with principal constituents.

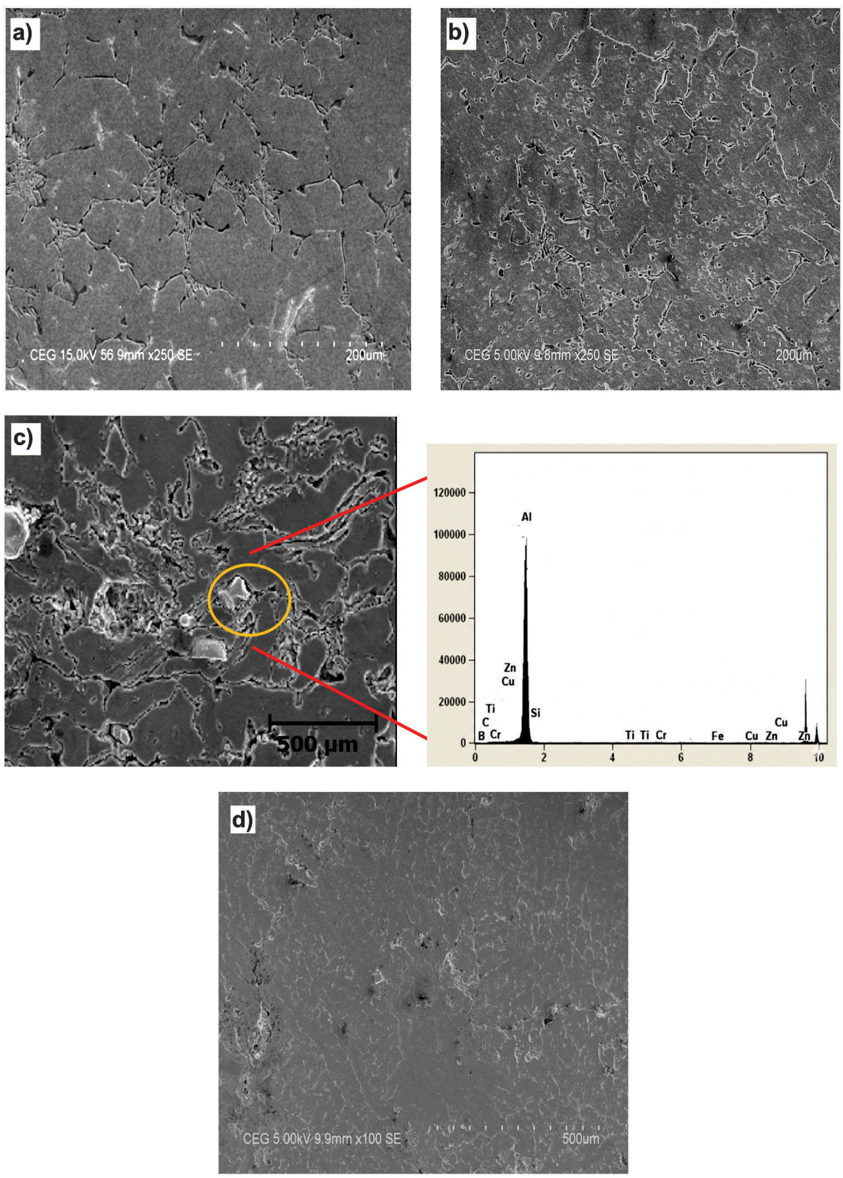

Figure 5. SEM and EDAX micrograph of AA7085 /TiB_2 Composites a) AA0, (b) AT3, (C) AT6, (d) AT9.

Figure 6 presents the XRD analysis of AA7085 subjected to T6 ageing at 230 °C. The diffraction pattern reveals only reflections corresponding to the α-Al matrix, signifying the absence of detectable secondary phases and the establishment of a supersaturated solid solution. There was no clear diffraction peaks linked to fine precipitates. It's due to Guinier–Preston (GP) zones and metastable η′ precipitates are so small, coherent, and have such a low volume fraction that they are below the XRD detection limit. But when the temperature was raised to 230 °C, low-intensity η ($MgZn_2$) reflections appeared, which showed that the precipitates were getting coarsening and the microstructure was changing to an aged state.

3.2. *Effect of heat treatment on hardness*

As shown in Figure 7, the hardness of the heat-treated samples increases with increasing solution temperature. At all heat-treated conditions, the hardness of the composites is higher than that of the base material. This improvement is mainly due to the strengthening effect of precipitation solidification and the cohesion of the particles in the aluminium (Al) matrix by the intermediate phase formed with it[24]. During heat treatment, significant changes occur in the microstructure of the material, particularly grain size, dislocation density, and phase distribution[25]. These changes directly influence the mechanical properties of the material. The increase in hardness with temperature is directly related to the phenomenon of solid solution hardening.

At higher solution temperature, solute atoms become more soluble in the matrix phase. This increases the solute–solvent atomic interaction, which in turn improves the overall strength and hardness of the material. In the initial stages of the ageing process, the increase in hardness is explained by particle diffusion. Further the local bonding strength and strain field interaction are strengthened. This significantly improves the mechanical properties of the material[26,27].

3.3. *Corrosion Behaviour of alloy and composites*

Figure 8 shows the corrosion rate of alloy and composites at varying immersion medium; its reveals increase in corrosion rate of AA0 at all conditions as compare to another fabricated composites and also in immersion duration. These changes are mainly due to ion diffusion and local concentration gradients. Diffusion processes play a key role in the stability and morphological evolution of the pit, as they control the transfer of ions at the edge of the pit[28]. In this process, the presence of a salt layer regulates the exchange of ions in and out of the pits surrounding the periphery. Furthermore, as immersion time increases, the continuous mass loss results from the uniform corrosion of the aluminium matrix.

The heat treatment of AA0 encourages aluminium (Al) atoms to form a solid solution within the α magnesium (Mg) phase. This slows down the corrosion rate at 48 hrs of immersion, however, when the exposure time is extended to 72 hours, the corrosion rate for AA0 rises significantly. Figures 9 show pictures of the composites before and after the immersion corrosion test, which was done with different amounts of NaCl solution. Notably, the AA0 sample exhibited greater corrosion compared to the other samples due to the absence of hard particle.

The corrosion behaviour of the alloy during ageing at 230 °C may be revealed, the alloy exposure to a chloride environment results in anodic dissolution and the initial formation of soluble aluminate species (AlO_2–), subsequently leading to the development of a surface film composed of Al_2O_3/Al $(OH)_3$. The stability of this film markedly affects corrosion rates and resistance to localized attack[29,30].

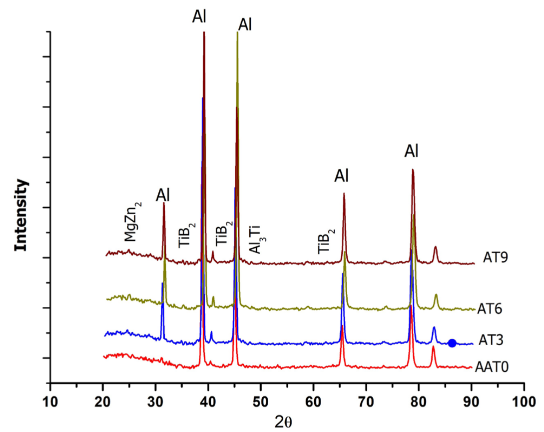

Figure 6. XRD analysis of AA7085 alloy and composites.

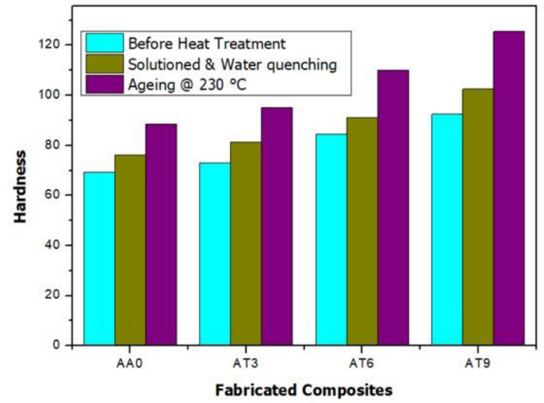

Figure 7. Mechanical Strength of Fabricated Material.

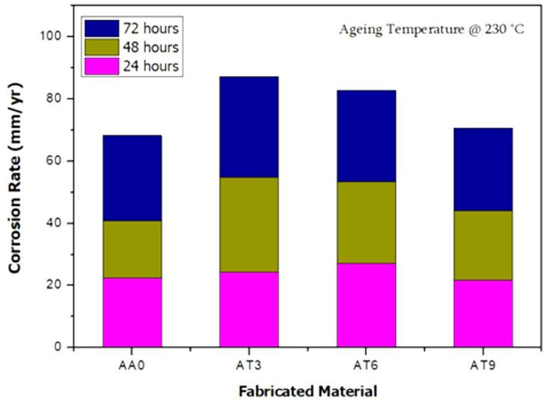

Figure 8. Corrosion rate at varying immersion duration.

AT3 and AT6 composites shows a higher corrosion rate as compare to AT9 composite. At lower TiB_2 particles limits the formation of stable and compact surface layer, as leads to easier access the matrix material to higher anodic dislocation and also its time depends in break down of passive Al_2O3 films, accumulation chloride ions at the affected region[31]. The mass loss rate increased progressively during longer immersion durations for low chloride concentrations. The observed increase is a result of the gradual and consistent dissolution of $AlO2^-$ ions from the parent surface, which prevents their precipitation as time progresses. In contrast, at higher concentrations, the dissolution rate of $AlO2^-$ ions exceeds the threshold much more quickly, resulting in the development of a strong structure to avoid corrosion its slows down the corrosion rate and material loss on AT9 composite. It is evident from the weight loss study that the AT9 specimen retained considerable weight. This may be an outcome of a favorable condition where homogeneous distribution of the ceramic particles (TiB_2) happened and the additional passivation layer that developed on the surface of the AT9 nanocomposites during exposure over various time periods.

Under artificial ageing conditions, rapid solute diffusion occurs at elevated temperatures, promoting the development of clusters and fine precipitates. At the nanoscale, this enhances the hardness of the composites, and XRD examination verifies the absence of bulk crystalline phases[32].

3.4. SEM analysis on corroded area

Figure 10 presents corroded specimens at 72 h immersion conditions. In Figure 10(a), the AA0 specimen exhibits a higher density of corrosion pits compared to the composite materials, with its surface showing extensive localized pits. Conversely, the AT3, AT6 and AT9 composites as shown in Figures 10(b-d) display relatively minor corrosion pits.

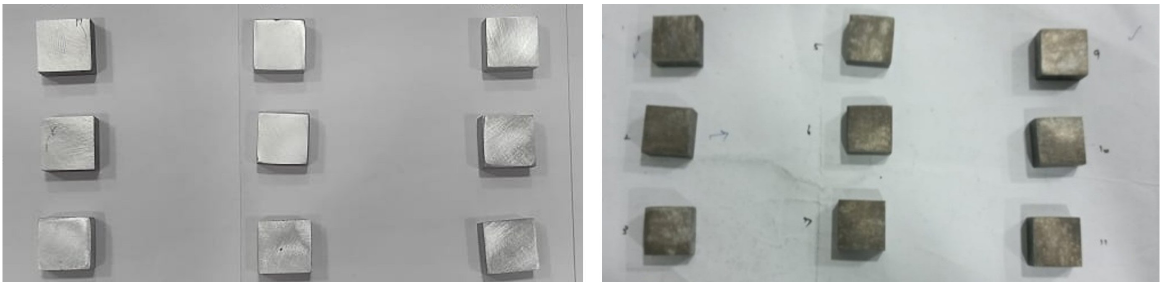

Figure 9. Before and After corrosion test samples of AT3, AT6 and AT9.

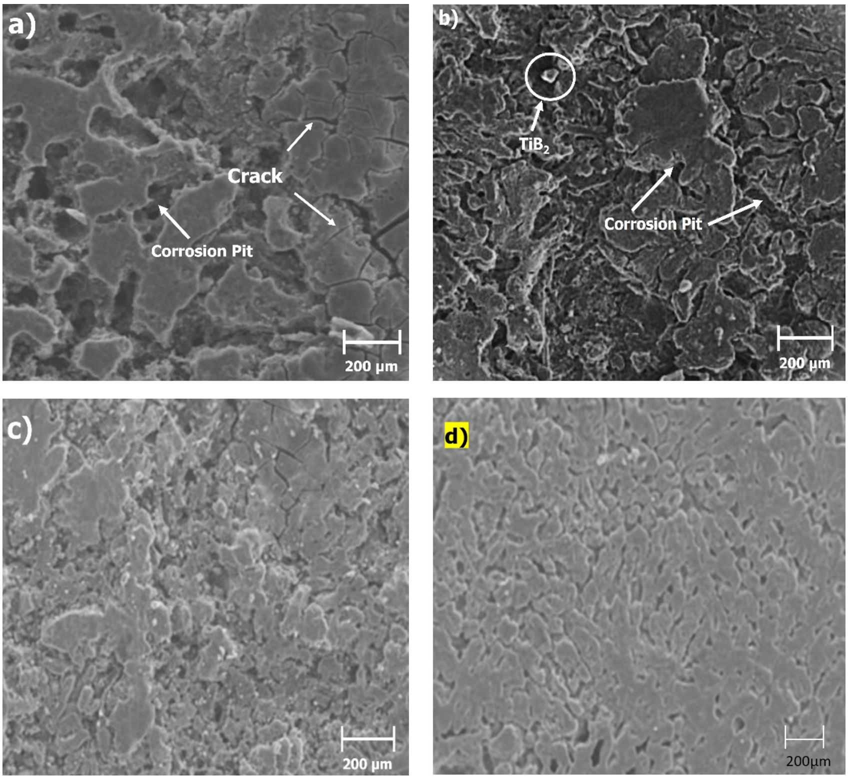

Figure 10. SEM micrograph of corroded samples after 72 hrs (a) AA0, (b) AT3, (c) AT6, (d) AT9.

SEM examination, as shown in Figure 10 of the corroded surfaces after immersion testing at peak-aged condition (230 °C) was carried out to identify pit morphology and the governing corrosion mechanism. The micrographs indicate localized pitting features with pit initiation preferentially occurring near grain-boundary precipitates and matrix–particle interfaces, which is characteristic of chloride-induced corrosion in Al–Zn–Mg–Cu alloys. Pits appear shallow to moderately deep without extensive intergranular cracking; thus, a predominantly micro-galvanic pitting mechanism exists rather than severe intergranular corrosion. Also, the much lower pit density seen in the higher-reinforcement composite (AT9) due to the uniform distribution of precipitates and chemically stable TiB_2 particles keep the passive film intact, as leads to the lower corrosion rate.

Over-ageing transpires via the coarsening of η′ to the equilibrium phase η($MgZn_2$), which leads to a reduction in the hardness of precipitates and dislocations, while augmenting electrochemical heterogeneity at grain boundaries, hence increasing localised corrosion. The presence of uniformly distributed, chemically stable TiB_2 particles contributes to temperature-stable strengthening mechanisms (load transfer, grain refinement, and Orowan bypassing), thereby enhancing the integrity of the passive film; consequently, composites with a higher TiB_2 weight percentage exhibit superior hardness and a comparatively reduced number of pits during immersion tests[33].

4. Conclusion

Aluminium Matrix composites with differing weight percentages of ultra-high-temperature ceramic (UHTC) particles, specifically titanium diboride (TiB_2), were produced using stir casting. The corrosion behavior of these materials was evaluated at aging temperatures. The results of this study are presented below.

1. The microstructure of solution treated samples exposed a homogeneous structure with precipitates at grain boundaries while the quantity of the precipitates increases with extended ageing time.
2. The incorporation of Ultra High-Temperature Ceramic (UHTC) particles significantly enhanced the hardness of the AA7085/TiB_2 composites relative to AA0. Notably, the AT9 composite demonstrated superior hardness, measuring 122 HV, under ageing conditions when compared to all other manufactured materials. This improvement can be attributed to increased densification and a reduction in grain size.
3. The AT9 composites exhibited superior corrosion resistance relative to other composites, maintaining this performance for up to 72 hours of exposure at an aging temperature of 230 °C due to formation of strong preventive structure to reduce corrosion rate.
4. The SEM image of the corroded AA7085/TiB_2 composite samples showed that pits and cracks while aging at 230 °C promotes development of intermetallic phases.

5. Acknowledgements

The authors acknowledge Anna University Chennai for providing access to their facilities and resources to conduct this research.

7. References

1. Swamy PK, Mylaraiah S, Gowdru Chandrashekarappa MP, Lakshmikanthan A, Pimenov DY, Giasin K, et al. Corrosion behaviour of high-strength Al 7005 alloy and its composites reinforced with industrial waste-based fly ash and glass fibre: comparison of stir cast and extrusion conditions. Materials. 2021;14(14):3929.
2. Kumar SS, Erdemir FATİH, Varol T, Kumaran ST, Uthayakumar M, Canakci A. Investigation of WEDM process parameters of Al–SiC–B_4C composites using response surface methodology. International Journal of Lightweight Materials and Manufacture. 2020;3(2):127-35.
3. Kumar A, Rana RS, Purohit R, Namdev A, Saxena KK. Optimization of dry sliding wear behavior of Si3N4 and Gr reinforced Al–Zn–Mg–Cu composites using taguchi method. J Mater Res Technol. 2022;19:4793-803.
4. Kumar SD, Ravichandran M. Synthesis, characterization and wire electric erosion behaviour of AA7178-10 wt.% ZrB_2 composite. Silicon. 2018;10(6):2653-62.
5. Gopalakrishnan S, Murugan N. Production and wear characterisation of AA 6061 matrix titanium carbide particulate reinforced composite by enhanced stir casting method. Compos, Part B Eng. 2012;43(2):302-8.
6. Palanivel R, Dinaharan I, Laubscher RF, Davim JP. Influence of boron nitride nanoparticles on microstructure and wear behavior of AA6082/TiB_2 hybrid aluminum composites synthesized by friction stir processing. Mater Des. 2016;106:95-204.
7. Khan AH, Shah SAA, Umar F, Noor U, Gul RM, Giasin K, et al. Investigating the microstructural and mechanical properties of novel ternary reinforced AA7075 hybrid metal matrix composite. Materials. 2022;15(15):5303.
8. Shivalingaiah K, Nagarajaiah V, Selvan CP, Kariappa ST, Chandrashekarappa NG, Lakshmikanthan A, et al. Stir casting process analysis and optimization for better properties in Al-MWCNT-GR-based hybrid composites. Metals. 2022;12(8):1297.
9. Basumatary J, Wood RJK. Synergistic effects of cavitation erosion and corrosion for nickel aluminium bronze with oxide film in 3.5% NaCl solution. Wear. 2017;376:1286-97.
10. El-Aziz KA, Saber D, Sallam HEDM. Wear and corrosion behavior of Al–Si matrix composite reinforced with alumina. J Bio Tribocorros. 2015;1:1-10.
11. Isadare AD, Aremo B, Adeoye MO, Olawale OJ, Shittu MD. Effect of heat treatment on some mechanical properties of 7075 aluminium alloy. Mater Res. 2013;16:190-4.
12. Suthar J, Patel K. Corrosion behaviour of Mg, graphite-, B4C and Ti-reinforced hybrid aluminium composites. Journal of The Institution of Engineers. 2022;103(4):689-704.
13. Kadaru SKR, Kannan M, Karthikeyan R. Preparation and investigation of wear and corrosion behaviour of Al 7475/CSA/Graphite hybrid metal matrix composites. Adv Mater Process Technol. 2024;10(4):2840-52.
14. Mahmoud TS, El-Kady ESY, Al-Shihiri ASM. Corrosion behaviour of Al/SiC and Al/Al2O3 nanocomposites. Mater Res. 2012;15:903-10.
15. Dhanapal A, Boopathy SR, Balasubramanian V, Zaman AT. Investigation of corrosion and metallurgical characteristics of friction stir-welded magnesium alloy welds under immersion, salt fog, pitting and galvanic corrosion tests. Metallurgical Research & Technology. 2013;110(6):373-89.
16. He X, Pan Q, Li H, Huang Z, Liu S, Li K, et al. Effect of artificial aging, delayed aging, and pre-aging on microstructure and properties of 6082 aluminum alloy. Metals. 2019;9(2):173.
17. Chen Q, Zhao W, Jiang J, Huang M, Li M, Wang Y, et al. Effect of T6 heat treatment on microstructure and mechanical properties of large-weight aluminum alloy flywheel housing parts formed by local-loading squeeze casting. J Mater Res Technol. 2023;24:612-1625.

18. Manickam D. Effect of solution heat treatment and artificial aging on compression behaviour of A356 alloy. Medziagoryra. 2019;25:281-5.
19. Liu B, Zhang X, Zhou X, Hashimoto T, Wang J. The corrosion behaviour of machined AA7150-T651 aluminium alloy. Corros Sci. 2017;126:265-71.
20. Sambathkumar M, Gukendran R, Vijayanand M. Investigation of corrosion behaviour of Al 7075/B4C/Al2O3 hybrid metal matrix composite. Mater Today Proc. 2022;50:1606-10.
21. Zhou J, Miao J, Wang B, Wang J. Effect of solution treatment and aging treatment on mechanical properties of 2060 Al-Li alloy and process multi-objective optimization. Metals. 2022;12:897.
22. Hou Y, Chen L, Li Z, Zhao G, Zhang C. Effects of artificial aging on microstructure, mechanical properties and stress corrosion cracking of a novel high strength 7A99 Al alloy. Mater Sci Eng A. 2020;780:139217.
23. He X, Pan Q, Li H, Huang Z, Liu S, Li K, et al. Effect of artificial aging, delayed aging, and pre-aging on microstructure and properties of 6082 aluminum alloy. Metals (Basel). 2019;9(2):173.
24. Mukund A, Nair AS, Nived S, Raagavendran R, Premkumar A, Raj AN, et al. Impact of solutionising temperature on the microstructure, hardness and tensile strength of Al-6.6 Si-0.3 Mg-3Ni alloys. Mater Today Proc. 2021;38:2117-22.
25. Sarker S, Haque MS, Alvy MSA, Abir MMH. The effects of solution heat treatment on the microstructure and hardness of an aluminum-4% copper alloy with added nickel and tin. Journal of Alloys and Metallurgical Systems. 2023;4:100042.
26. Jin BR, Ha DW, Jeong CY. Effect of solution treatment on the hardness and tensile properties of Al–Mg–Si alloys for automotive chassis. Mater Trans. 2019;60(5):815-23.
27. Maier P, Steinacker A, Clausius B, Hort N. Influence of solution heat treatment on the microstructure, hardness and stress corrosion behavior of extruded Resoloy. JOM. 2020;72:1870-9.
28. Hou Y, Chen L, Li Z, Zhao G, Zhang C. Effects of artificial aging on microstructure, mechanical properties and stress corrosion cracking of a novel high strength 7A99 Al alloy. Mater Sci Eng A. 2020;780:139217.
29. Frankel GS. Pitting corrosion of metals: a review of the critical factors. J Electrochem Soc. 1998;145(6):2186.
30. Birbilis N, Buchheit RG. Electrochemical characteristics of intermetallic phases in aluminum alloys: an experimental survey and discussion. J Electrochem Soc. 2005;152(4):B140.
31. Li K, Wang Z, Wang F, Geng J, Li Y, Xia P, et al. Different effects of TiB2 particles on corrosion behaviors of in-situ TiB2/7075 composites in active and passive environments. Corros Sci. 2024;235:112201.
32. Hsiao TJ, Chiu PH, Tai CL, Tsao TC, Tseng CY, Lin YX, et al. Effect of Cu additions on the evolution of eta-prime precipitates in aged AA 7075 Al–Zn–Mg–Cu alloys. Metals. 2022;12(12):2120.
33. Manojkumar S, Mehta KK. Effect of TiB_2 on mechanical and corrosion properties of Al 7075/TiB_2/Gr composite prepared by stir casting. Mater Today Proc. 2023;91:62-6.

Data Availability

The data that support the findings of this study shall be obtained from the corresponding author upon request.